In celebration of the 60th birthday of Dr. Andrew K. Galwey

A THERMOANALYTICAL STUDY OF THE OXIDATION OF CHALCOCITE

J. G. Dunn[1], A. R. Ginting[1] and B. O'Connor[2]

[1]School of Applied Chemistry
[2]Department of Applied Physics Curtin University of Technology, Perth, Western Australia

Abstract

A sample of chalcocite of particle size 45–75 μm has been oxidised in a TG-DTA apparatus at a heating rate of 10 deg·min^{-1} and the products at various temperatures characterised by XRD, SEM, FTIR and EPMA. This has enabled the events in the TG-DTA record to be assigned to specific chemical reactions, as well as the development of a full reaction scheme for the oxidation of chalcocite.

Only minor reactions occurred up to 430°C, but above this temperature there was significant oxidation which resulted in an exotherm and mass gain. These events were due primarily to the oxidation of sulfide to copper(I) oxide, and the formation of copper(II) sulfate. The reaction then slowed, but melting commenced at 490°C which permitted further oxidation to take place with the appearance of a second exotherm and mass gain. By 570°C, sulfide oxidation was complete, but solid-solid reactions took place between Cu_2O and $CuSO_4$ to produce $CuO \cdot CuSO_4$. Some conversion of Cu_2O had occurred. By 775°C, CuO and $CuO \cdot CuSO_4$ were the only phases detected. Above this temperature the latter phase was unstable and decomposed to the end product CuO.

Keywords: electron probe microanalysis oxidation of chalcocite, FTIR, hot stage microscopy, SEM, TG-DTA, X-ray

Introduction

Chalcocite Cu_2S, is one of a number of identifiable compounds in the copper-sulfur system which also includes covellite (CuS), analite ($Cu_{1.75}S$), digenite ($Cu_{1.8}S$), and djurleite ($Cu_{1.96}S$) [1–3]. Chalcocite is one of the most important sources of copper, and occurs principally as a supergene mineral in the enriched zone of sulfide deposits [4].

A limited number of studies have been reported on the oxidation of chalcocite. Some major reactions have been identified. The oxidation roasting of chalcocite in air occurs in the temperature range from 420 to 550°C [5]. The phases

present in the product after roasting at 490°C for 9 minutes were digenite and copper(I) oxide. The use of DTA and TG methods to study the oxidation of chalcocite has also been reported. Exothermic peaks occurred at 470, 560 and 620°C, while endothermic peaks appeared at 835 and 1080°C [6]. By TG, a mass gain has been noted at 340 to 380°C [7], and is related to the formation of copper(II) sulfate.

In this paper, the oxidation behaviour of chalcocite from 25 to 1000°C is determined by using various techniques including simultaneous thermo-gravimetry-differential thermal analysis (TG-DTA), X-ray diffraction (XRD), scanning electron microscopy (SEM), Fourier transform infrared (FTIR) spectroscopy, electron probe micro-analysis (EPMA), hot stage microscopy (HSM), and wet chemical analysis. These techniques allow qualitative and quantitative information on the progress of the oxidation reaction as a function of temperature.

Experimental

Sample preparation

A quantity of a natural chalcocite (15 g) was obtained from Ward Company, USA. It was ground in a mortar and sieved through Endicott test sieves using a Ro-Tap testing sieve shaker. In this study, all work was on the 45–75 μm fraction which was stored in a vacuum desiccator when not under test.

Techniques

Simultaneous TG-DTA measurements were performed using a Stanton Redcroft 780 Thermal Analyser and IBM microcomputer interface. Approximately 5 mg of sample was weighed into an alumina crucible (3.8 mm internal diameter and 3.0 mm in height) and placed in the TG-DTA apparatus. A gas flow of 35 ml·min^{-1} was set. The sample was heated at 10 deg·min^{-1}. The atmosphere used included air and oxygen flowing through a silica gel scrubber to remove water, and nitrogen flowing through an oxygen scrubber. All the gases were industrial grade.

XRD experiments were performed using a Siemens D500 Bragg-Brentano diffractometer consisting of a copper X-ray tube, rotating specimen stage and a sodium iodide detector. The machine settings were 40 kV, 30 mA and the CuK$_\alpha$ line was used with a graphite monochromator. The detector angle was in the range 10–100° with a goniometer step at 0.04°. Time counting was one sec-

ond. X-ray patterns were processed with the EVA program marketed by So-cabim, SARL a bis, Villa du Bell Air, Paris.

FTIR spectra were recorded with a Perkin Elmer 1720 FTIR Spectrometer with a TGS detector. 10 scans were applied on each sample at a mirror velocity of 0.2 $cm \cdot s^{-1}$ and a resolution of 4 cm^{-1} throughout the range 4000 to 400 cm^{-1}. The spectra were obtained on 1 mg samples dispersed in 199 mg KBr and pressed into a disk. The spectra were analysed using IRDM software.

SEM data were collected from representative samples embedded in epoxy resin. The micrographs of the polished section samples, coated with carbon, were taken using a JEOL JSM-35C instrument fitted with an X-ray energy dis-persive spectrometer (EDS-Si(Li) detector).

Backscattered electron images were collected using an accelerating voltage of 25 keV. The micrographs and the images of the polished section sample without coating were determined under a Nikon Labhot-2 optical microscope with a NCB filter. Element analysis was carried out with by energy dispersive spectrometry (EDS).

EPMA was performed on carbon coated, polished sections using a Cameca SX-50 Electron Probe and wavelength dispersive spectrometers. Data were processed by ANU/CSIRO WANU-SX Software V 7.03. Analyses were per-formed at an accelerating voltage of 20 kV and a beam current of 30 nA. Chal-copyrite and copper metal standards were employed. A manual and step scanning system were used to analyse approximately 30 particles.

HSM was carried out in a Linkam 1500 hot stage controlled by the Linkam TMS90 temperature programmer. Events were observed with a Nikon Labhot-2 microscope and recorded on video camera. A mixture of the solid components was placed in the crucible and heated at 10 $deg \cdot min^{-1}$ in the appropriate atmo-sphere.

Results and discussion

Sample characterization

The results of wet chemical analysis of chalcocite are given in Table 1. The data indicated that the chalcocite had a purity of >99%. Analysis of 30 particles of chalcocite by EPMA showed that there was no significant variation in parti-cle-to-particle composition, and the atomic ratio of Cu:S was confirmed as 2:1. Minor quantities of Si, K and Na were found by EDS while the presence of Fe was indicated by EPMA. Low chalcocite was the only phase detected by XRD.

Table 1 Copper and sulfur content of the chalcocite determined by wet chemical analysis

	Composition /%		
Sample	Cu	S	Total
1	78.7	20.5	99.2
2	78.6	20.5	99.1

A back scattered electron image obtained from SEM of unreacted chalcocite is shown in Fig. 2a. The particles are angular and fractures are apparent on the surface. Optical microscopy revealed a shiny metallic appearance.

Oxidation experiments

A typical TG-DTA trace for the oxidation of chalcocite is shown in Fig. 1. Mass gains were evident in the temperature ranges 425–510°C and 510–560°C. From 560°C the mass gain increased at a slower rate up to 725°C. A mass loss occurred between 725° and 810°C.
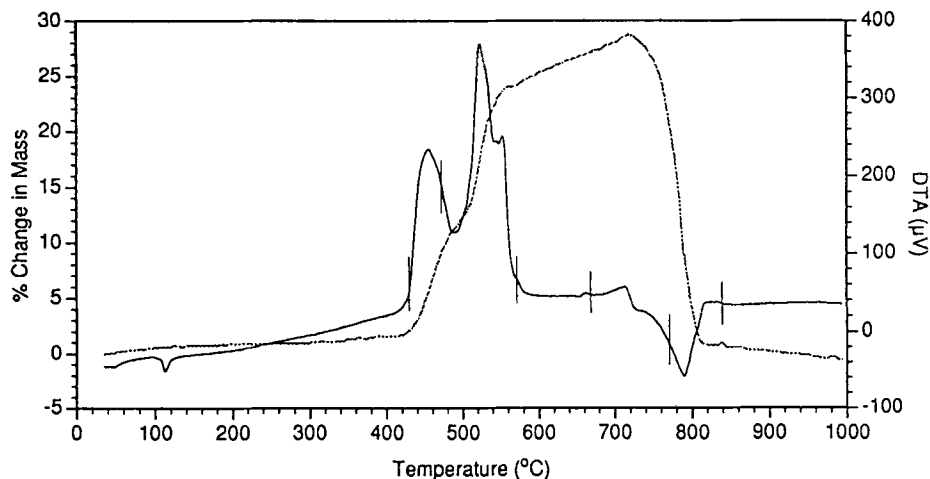
Fig. 1 TG-DTA curve for the oxidation of chalcocite. The vertical lines indicate the temperatures at which partially oxidised samples were taken for analysis. 5 mg sample, 10 deg·min^{-1} heating rate, air atmosphere, particle size 45–75 μm

Two endothermic peaks were present in the DTA record (Fig. 1) in the temperature ranges 107–117°C and 720–810°C. The first endotherm has no associated mass loss. This peak can be assigned to the transformation of orthorhombic to hexagonal chalcocite [1, 2, 8]. Two exothermic peaks occurred
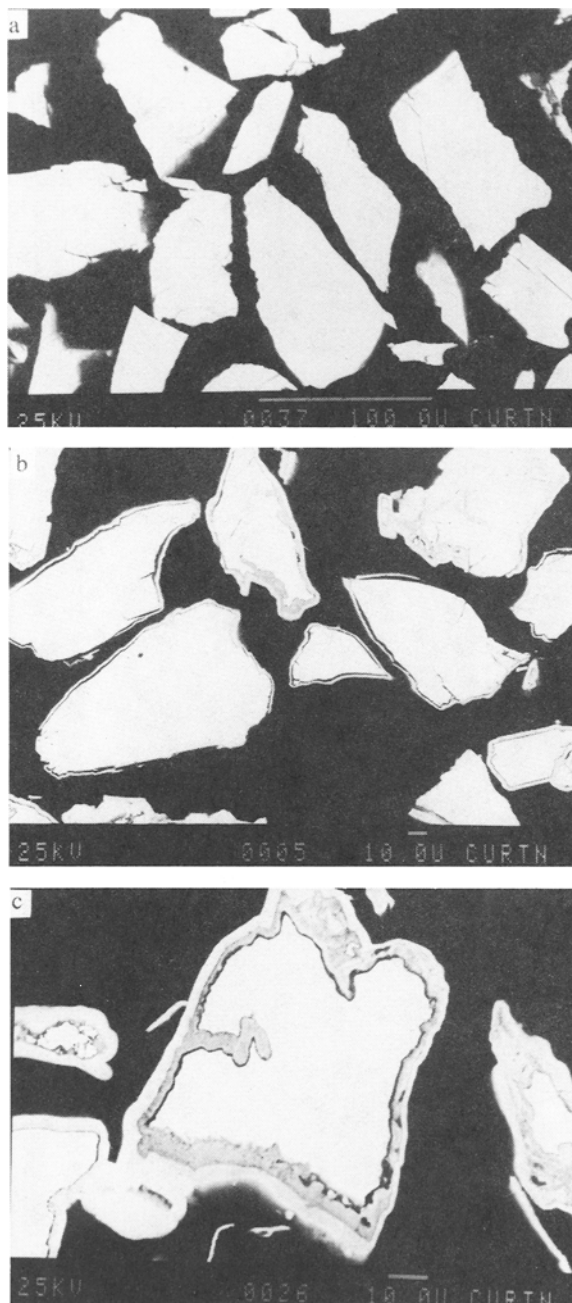
Fig. 2 Backscattered electron images of partially oxidised samples of chalcocite. Numbers indicate temperatures (in °C) at which samples were taken. (a) unreacted (b) 435 (c) 470
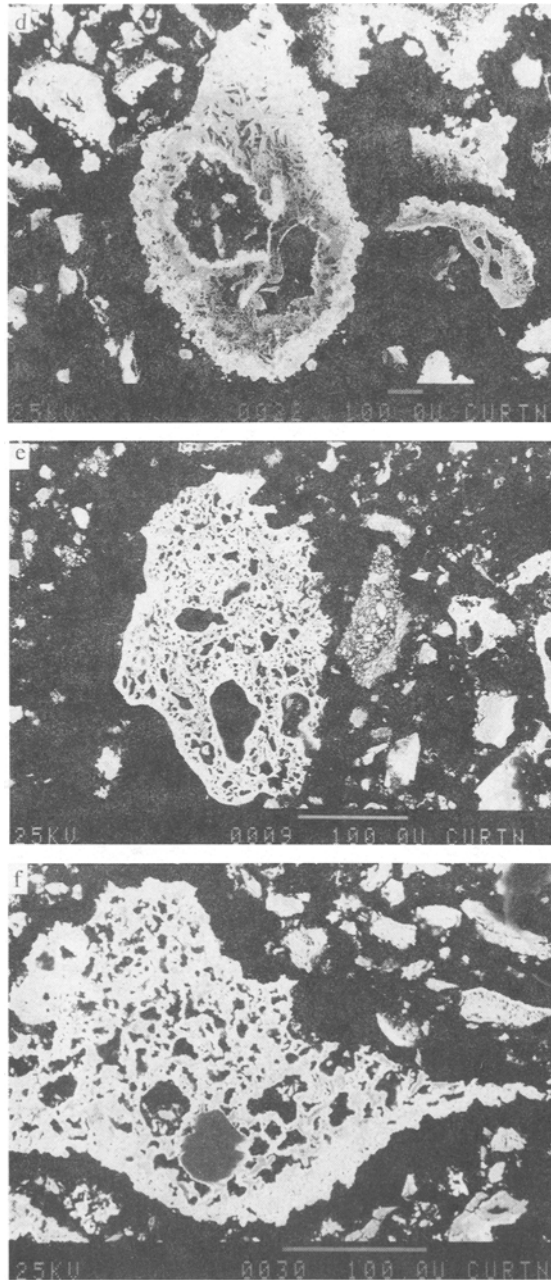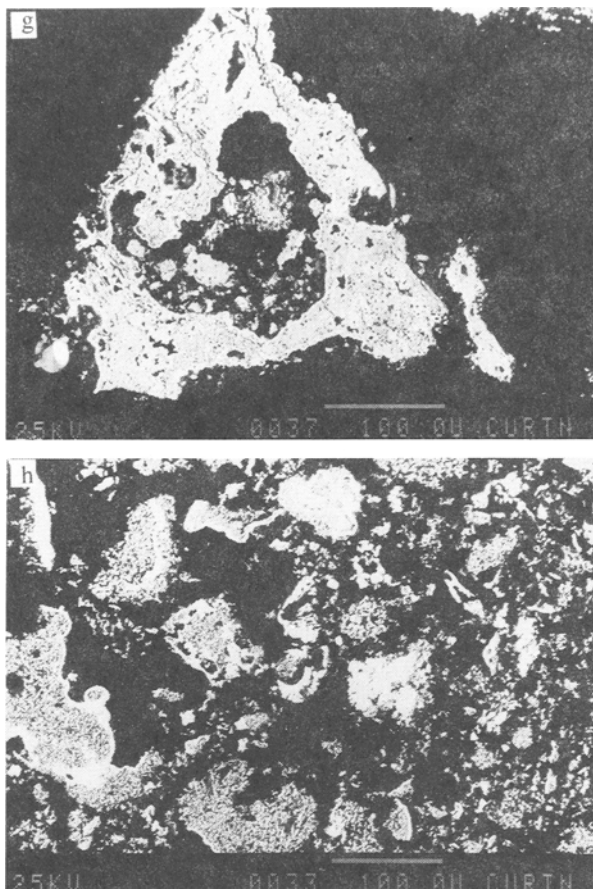
Fig. 2 Backscattered electron images of partially oxidised samples of chalcocite. Numbers in-
dicate temperatures (in °C) at which samples were taken. (d) 510 (e) 570 (f) 670

Fig. 2 Backscattered electron images of partially oxidised samples of chalcocite. Numbers indicate temperatures (in $^{\circ}$C) at which samples were taken. (g) 775 (h) 840

Table 2 Phases identified by XRD in partially oxidised chalcocite

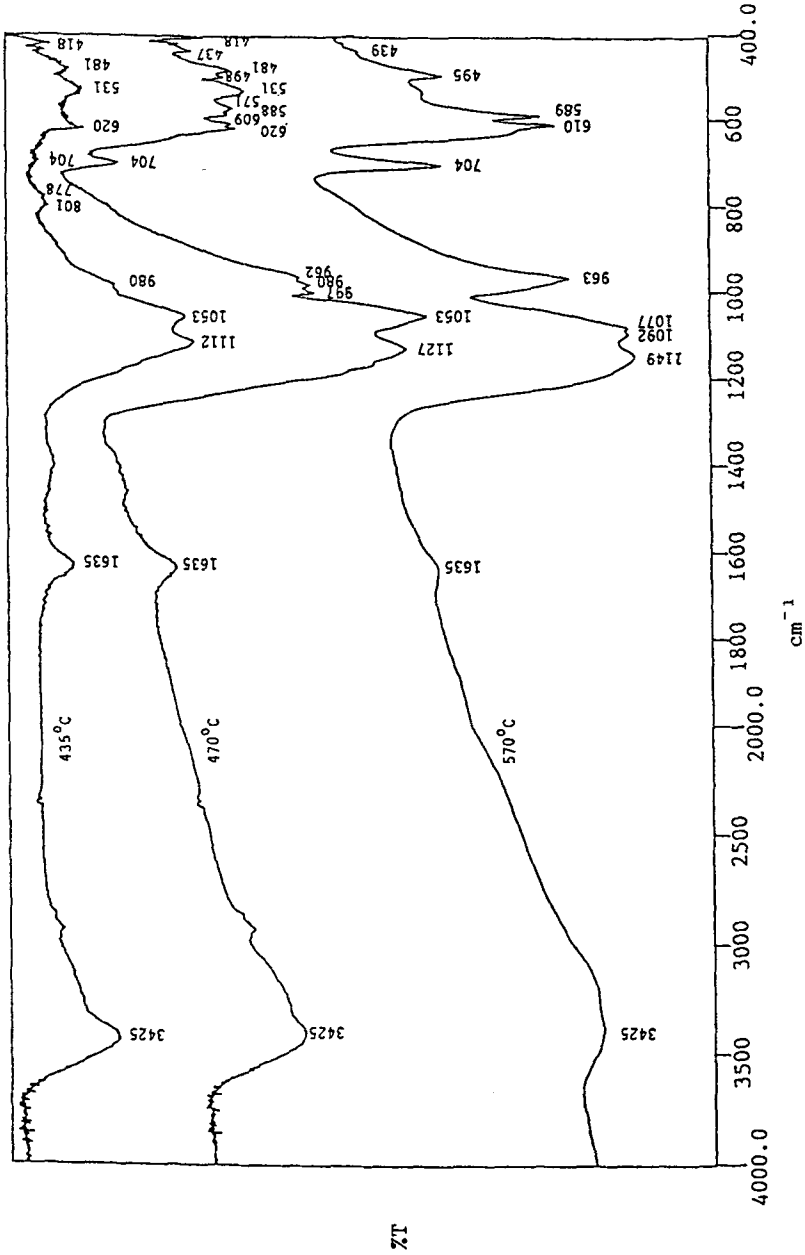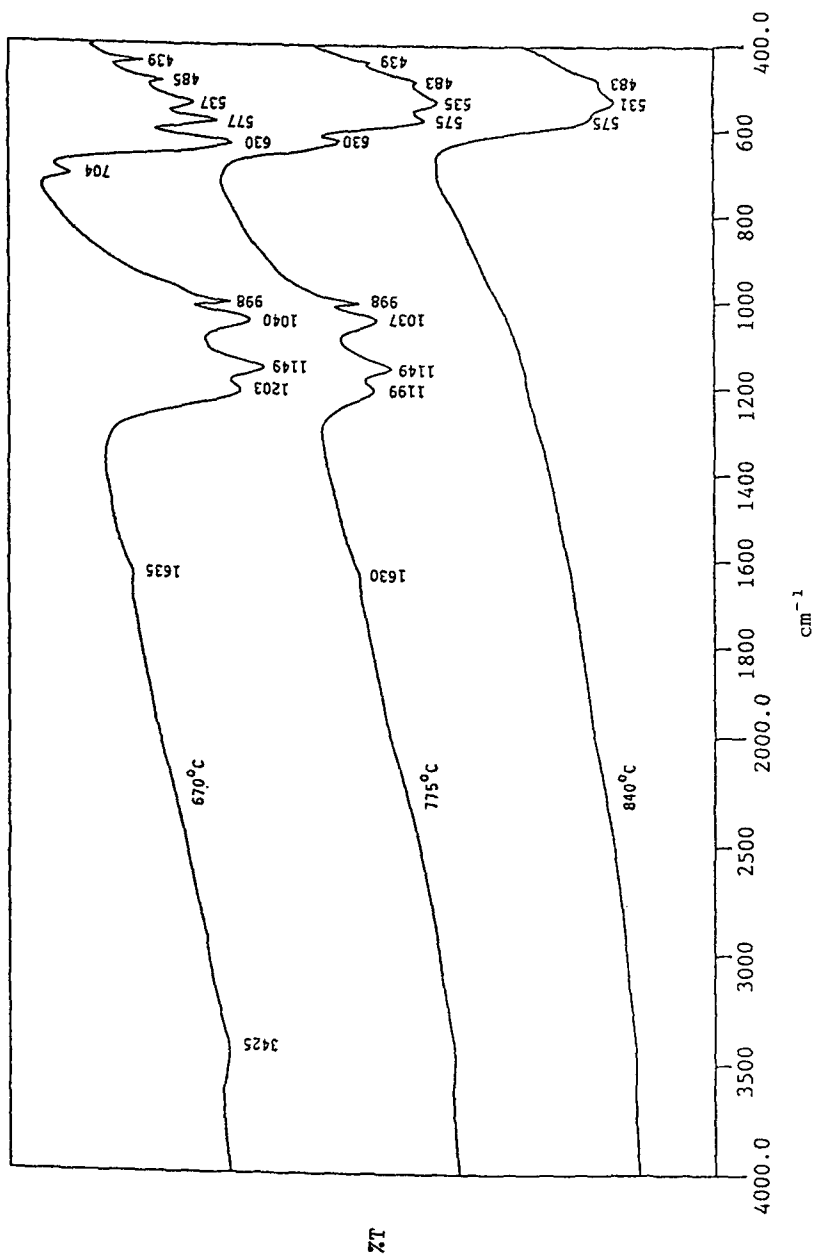| Temperature/$^{\circ}$C	Phase present
435	Cu_2S, $Cu_{1.96}S$, $Cu_{1.8}S$, and Cu_2O
470	Cu_2S, $Cu_{1.96}S$, $Cu_{1.8}S$, Cu_2O, and $CuSO_4$
570	Cu_2O, and $CuSO_4$
670	Cu_2O, $CuSO_4$, $CuO \cdot CuSO_4$, and CuO
775	$CuO \cdot CuSO_4$, and CuO
840	CuO

Fig. 3a

Fig. 3b FTIR spectra of partially oxidised chalcocite samples. 0.5% sample dispersed in KBr disc

in the temperature ranges 425–490°C and 490–585°C, and were associated with the first two mass gains.

Partially oxidised products were collected at selected temperatures, as shown in Fig. 1. The exothermic or endothermic peaks in the DTA trace were used as indicators of the beginning or end of a reaction. When the selected temperature was reached, the heating was stopped and air substituted by nitrogen.

Table 3 Quantitative EPMA of partially oxidised chalcocite particles heated to 470°C. Heating rate 10 deg·min^{-1}; air atmosphere

No. of particle	Grey rim/ mass%		Black rim/ mass%		Centre/ mass%	
	Cu	S	Cu	S	Cu	S
1	69.89	2.27	60.59	7.22	80.01	20.51
2	70.34	4.21	51.88	12.13	79.69	20.51
3	72.31	1.19	50.33	11.96	79.22	20.97
4	70.92	3.82	52.90	12.46	79.23	20.96
5	73.94	1.02	51.03	11.01	79.12	20.93
Total	357.40	12.51	266.73	54.78	397.27	103.88
Average	71.48	2.50	53.35	10.96	79.45	20.78
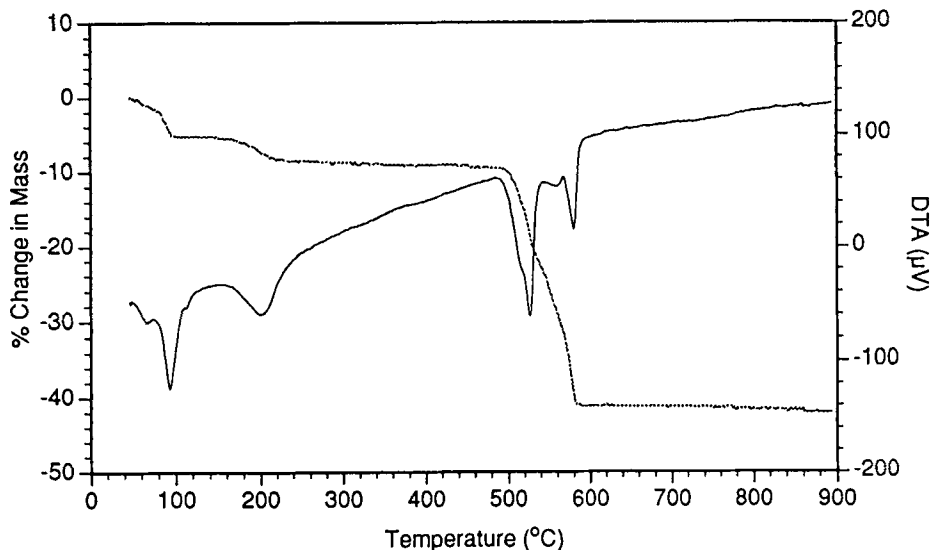
Fig. 4 TG-DTA trace of a mixture of Cu$_2$S and CuSO$_4$ (1:1 mass ratio) heated in nitrogen at 10 deg·min^{-1}.
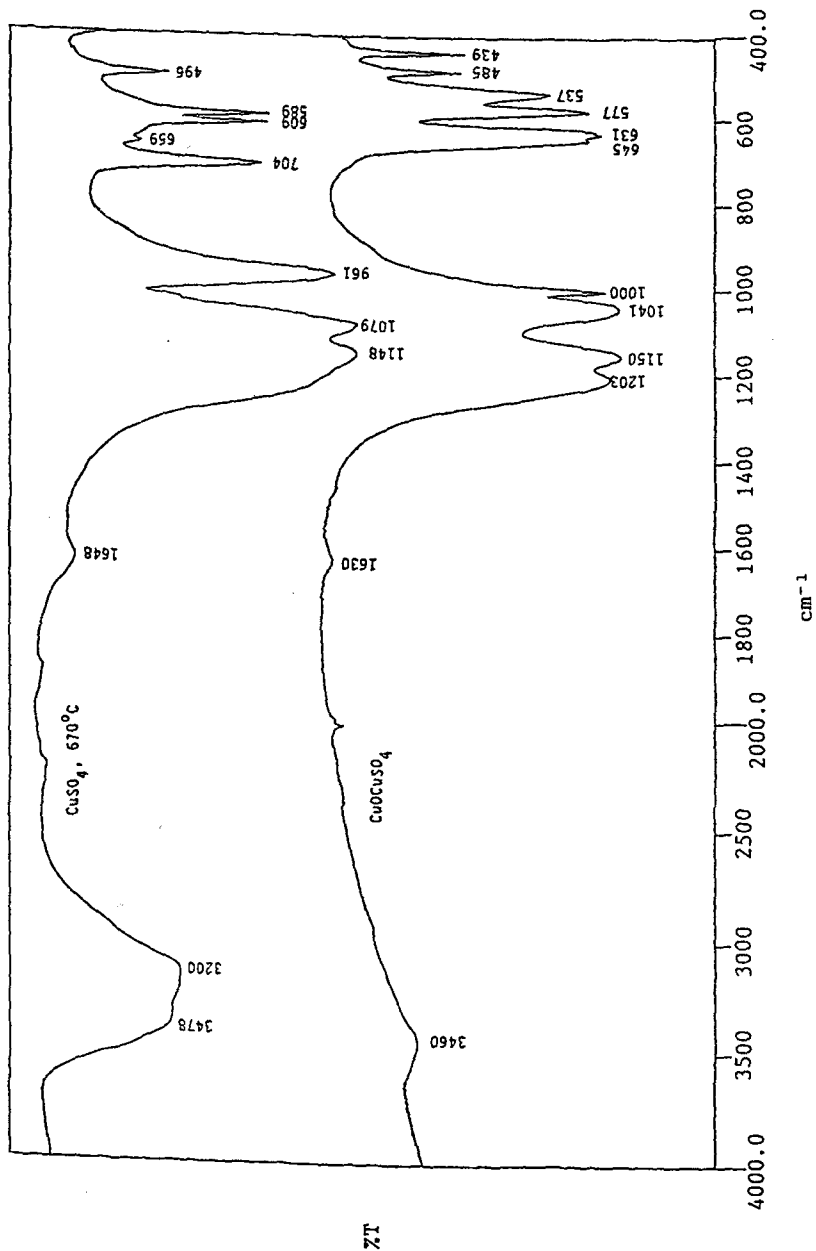
Fig. 5 FTIR spectra of $CuSO_4$ and $CuO.CuSO_4$

The material was then cooled and analysed by various techniques including XRD (Table 2), FTIR, SEM and EPMA (Table 3).

Backscattered electron (BSE) images, obtained on the SEM, of partially oxidised products taken at 435, 470, 570, 670, 775 and 840°C are given in Figs 2(b)-(g), respectively. FTIR spectra of the same samples are shown in Figs 3a and 3b, and FTIR spectra for $CuSO_4$ and $CuO \cdot CuSO_4$ in Fig. 5.
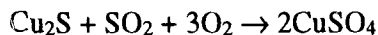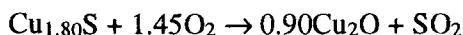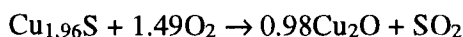
Reaction sequence

The oxidation behaviour of chalcocite in the temperature range 430 to 1000°C can be described in four stages. Firstly, there is the initial formation of oxidation products in the temperature range 430–490°C. The sample taken at 435°C, before any main events in the TG-DTA trace became apparent, nevertheless showed some evidence of oxidation. SEM micrographs (Fig. 2b) indicated the formation of a dense grey phase which occurred as a rim around the particles. Using image analysis, the thickness of the rim was measured to be up to 2 μm. The presence of Cu_2O was confirmed by XRD (Table 2). The most likely explanation for the grey rim is that it is copper(I) oxide formed by surface oxidation of chalcocite. Some sulfur deficient copper(I) sulfides were also detected by XRD.

Although the presence of copper(II) sulfate in the partially oxidised product at 435°C was not detected by XRD, the presence of this phase was evident in an FTIR spectrum (Fig. 3a). One of the sample peaks at 704 cm^{-1} was coincident with one of the characteristic peaks of copper(II) sulfate [9]. The inability of XRD to detect the presence of copper(II) sulfate could be due to the very low concentration formed. In some particles, optical microscopy revealed that, in addition to the grey phase, a second black product was present.

At 470°C, two rims were apparent around all the particles (Fig. 2c). The outer rim was the grey phase, as previously indicated at 435°C, while a black phase was apparent as an inner rim. The thicknesses of the grey and the black phases varied from 4 to 10 μm. Quantitative EPMA results for five particles are given in Table 3, and show that the atom composition of this grey phase was rich in copper and very low in sulfur. Calculations from the EPMA data give a Cu value which is too low to correspond exactly with Cu_2O, whereas the centre of the particle corresponded to unreacted Cu_2S. This grey phase must be predominantly copper(I) oxide intermixed with some unreacted or partially reacted sulfide phase. The black phase was porous. EPMA results (Table 3) gave Cu and S contents which are intermediate between those obtained for Cu_2O and Cu_2S, but which did not conform to either of the two possible copper sulfate phases. The XRD pattern clearly identified $CuSO_4$ as one of the components of

the sample at 470°C, and the sulfate bands were strongly evident in the FTIR spectrum (Fig. 3a). Optical microscopy showed that some oxide was included in the black rim, so that, again, the rim was at least a binary mixture. This would account for the low S value relative to pure $CuSO_4$ (EPMA data S = 12%, calculated for $CuSO_4$ = 20.1%) and the high copper value relative to pure $CuSO_4$ (EPMA data Cu = 52%, calculated for $CuSO_4$ = 40%).

The mass gain in the TG trace started at 430°C. This is due to the formation of copper(II) sulfate. Thornhill and Pidgeon [5] reported that the formation of this compound occurred at 490°C when chalcocite was roasted in an air atmosphere. On the evidence collected, the reaction sequences in the temperature range 430–490°C are:

$$Cu_2S + 0.01O_2 \rightarrow Cu_{1.96}S + 0.02Cu_2O$$

$$Cu_2S + 0.05O_2 \rightarrow Cu_{1.80}S + 0.10Cu_2O$$

$$Cu_{1.96}S + 1.49O_2 \rightarrow 0.98Cu_2O + SO_2$$

$$Cu_{1.80}S + 1.45O_2 \rightarrow 0.90Cu_2O + SO_2$$

$$Cu_2S + SO_2 + 3O_2 \rightarrow 2CuSO_4$$

The first major exotherm can be assigned to the third and fourth reactions, since the formation of SO_2 is highly exothermic.
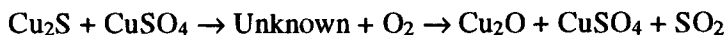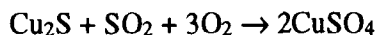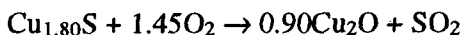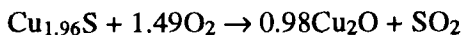
The second exotherm and mass gain occurs in the temperature range 490 to 590°C. In this range the solid material melts, as evident from the solidified mass present in the cooled crucible. BSE images of samples taken at 510 and 570°C show that the shapes of the particles have changed, and in some cases there is evidence of needle-like crystals (Fig. 2d and 2e). Only Cu_2O and $CuSO_4$ were detected by XRD. TG-DTA experiments, conducted with a mixture of chalocite and $CuSO_4 \cdot 5H_2O$ in nitrogen, gave the trace shown in Fig. 4. The low temperature endotherms and mass losses are due to the loss of the water of crystallisation associated with the copper(II) sulfate. The endotherm commencing at 490°C may be due to melting although the mass loss also indicates that a reaction is taking place. This temperature agrees with the melting temperature reported by Jacinto, Nagamori and Sohn [10], who used sealed tube methods to study the reaction. The second endotherm and mass loss commence at 570°C. The experiment was repeated in a hot stage microscope, where it could be seen that the mixture reacted vigorously, in a similar temperature range, with gas evolution and melting. Heating chalocite alone in a nitrogen atmosphere does not show any reaction or the melting process. Since the micrographs and EPMA data of the partially oxidised chalocite just prior to this

temperature range (Fig. 2b and Fig. 2c) show that the individual particles contain unreacted chalcocite in contact with $CuSO_4$, reaction between these two solid phases is clearly possible.

Rosenqvist [11] has reported that there is a solid-solid reaction between Cu_2S and $CuSO_4$ which produces a melt which exists in the temperature range 450–550°C. He attributes this to the formation of a ternary eutectic reaction between chalcocite, copper(I) oxide, and copper(II) sulfate. He also reports that Nagamori and Habashi [12] attribute the melting phenomena to the formation of Cu_2SO_4. Measurements on the melting point of Cu_2SO_4 failed initially because the substance decomposed before melting, but in a sealed tube in an SO_2 atmosphere it melted at 423°C [10]. More recently it has been reported [13] that Cu_2SO_2 may be the molten substance in this temperature range. The evidence is not conclusive or confirmed for any of the three propositions. There has been no explanation given for the appearance of the second endotherm.

FTIR spectra could also be used to follow the appearance of $CuO \cdot CuSO_4$. There are several peaks in Fig. 5 which are characteristic of the phase, for example at 1041, 1000, 631, 577, 537 and 439 cm^{-1}, and which are not interfered with by the bands from $CuSO_4$. The FTIR spectrum at 570°C (Fig. 3a) shows a small peak at 439 cm^{-1} which is indicative of the formation of $CuO \cdot CuSO_4$, although this phase was not detected by XRD. Hence the formation of this phase commences as low as 570°C.

The reaction sequences in the temperature range 490–590°C can be considered to be the continuation of the oxidation of the remaining sulfides, which accounts for the second exotherm, and the formation of $CuSO_4$, which accounts for the second mass gain.

$$Cu_2S + 0.5O_2 \rightarrow Cu_2O$$

$$Cu_{1.96}S + 1.49O_2 \rightarrow 0.98Cu_2O + SO_2$$

$$Cu_{1.80}S + 1.45O_2 \rightarrow 0.90Cu_2O + SO_2$$

$$Cu_2S + SO_2 + 3O_2 \rightarrow 2CuSO_4$$

$$Cu_2S + CuSO_4 \rightarrow Unknown + O_2 \rightarrow Cu_2O + CuSO_4 + SO_2$$

The formation of $CuO \cdot CuSO_4$ can take place by two possible routes, according to the equations:

$$2CuSO_4 \rightarrow CuO \cdot CuSO_4 + SO_2 + 0.5O_2$$

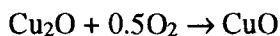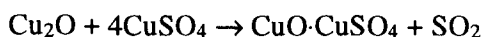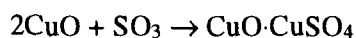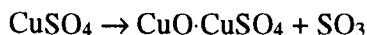$$Cu_2O + 4CuSO_4 \rightarrow 3CuO \cdot CuSO_4 + SO_2$$
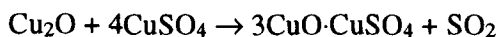
Since both phases are present in the sample at 570°C, either route is possible.

In the third region, from 590 to 725°C, the formation of copper(II) oxysulfate continued, and was detected by both FTIR (Fig. 3b) and XRD (Table 2). Copper(I) oxide is oxidised to copper(II) oxide by 670°C. Although in this temperature range SO_3 is evolved in the formation of copper(II) oxysulfate, no mass loss appears in the TG trace. Instead a gradual mass gain occurs. This is probably because of the reaction between CuO and SO_3 to form copper(II) oxysulfate, and the oxidation of Cu_2O to CuO. Some loss of porosity in the particles had occurred (Fig. 2f and 2g) which may be due to the formation of the new phases or the recrystallisation of existing phases.

The reactions proposed for the temperature range 590–725°C are given below.

$$CuSO_4 \rightarrow CuO \cdot CuSO_4 + SO_3$$

$$2CuO + SO_3 \rightarrow CuO \cdot CuSO_4$$

$$Cu_2O + 4CuSO_4 \rightarrow CuO \cdot CuSO_4 + SO_2$$

$$Cu_2O + 0.5O_2 \rightarrow CuO$$

The final stage is the decomposition of copper(II) oxysulfate to CuO between 725 and 820°C and accounts for the final mass loss and the endotherm.

Conclusions

The reaction scheme for the oxidation of chalcocite has been established. In general, no significant oxidation occurs below 430°C, although a dense oxide rim is formed around individual particles. The first exotherm, which occurs between 430–490°C, is due to the partial oxidation of the sulfide species. The mass gain is due to the formation of $CuSO_4$ which occurs as a second rim inside the oxide rim. The return of the first exotherm towards the baseline at 490°C and the decrease in the rate of mass gain suggest that the oxidation reaction has been retarded. This may be due to the formation of the oxide and sulfate rims, particularly the dense outer oxide rim, inhibiting the diffusion of oxygen into the core material. The melting process which occurs at 490°C would remove, or at least reduce, this barrier and so the oxidation process can proceed to completion, and give rise to the second exotherm and mass gain. These reactions are complete by 570°C.

Above 570°C, $CuSO_4$ decomposes to form $CuO \cdot CuSO_4$ and the liberated SO_3 combines with oxide to form more $CuO \cdot CuSO_4$. Oxidation of Cu_2O also contributes to the slow mass gain. Above 775°C, the sulfate decomposes to leave CuO as the end product.

*   *   *

References

1 N. W. Buerger, Econ. Geol., 36 (1941) 19.

2 E. H. Roseboom, Econ. Geol., 61 (1966) 649.

3 N. R. Serebryanaya, Geochem. Int., 3 (1966) 687.

4 C. Palache, H. Berman and C. Frondel, The System of Mineralogy, Vol. 1, John Wiley and Son, New York 1966 p. 189.

5 P. G. Thornhill and L. M. Pidgeon, J. Metal., (1957) 992.

6 R. Dimitrov and B. Boyanov, Thermochim. Acta, 64 (1983) 31.

7 G. W. Reimers and K. E. Hjelmstad, US Bureau of Mines Report of Investigations 9118 (1987) pp.15.

8 B. J. Skinner, Econ. Geol., 65 (1970) 724.

9 A. Hezel and S. D. Ross, Spectrochim. Acta, 22 (1966) 1949.

10 N. Jacinto, M. Nagamori and H. Y. Sohn, Metall. Trans., 13B (1982) 515.

11 T. Rosenqvist, Metall. Trans., 9B (1978) 337.

12 M. Nagamori and F. Habashi, Metall. Trans., 5 (1974) 523.

13 H. Debinski and J. Walczak, J. Thermal Anal., 29 (1984) 977.

Zusammenfassung — Eine Chalkozitprobe der Partikelgröße 45–47 µm wurde in einem TG-DTA-Gerät bei einer Aufheizgeschwindigkeit von 10 deg·min^{-1} oxidiert und die Produkte bei verschiedenen Temperaturen mittels XRD, SEM, FTIR und EPMA charakterisiert. Dies ermöglichte die Zuschreibung verschiedener Verläufe in der TG-DTA-Aufnahme zu spezifischen chemischen Reaktionen. Weiterhin ermöglichtes es die Erstellung eines umfassenden Reaktionsschemas für die Oxidation von Chalkozit.

Bis 430°C treten nur Minor-Reaktionen auf, aber oberhalb dieser Temperatur gibt es eine deutliche Oxidation mit einer Exothermen und Massenzuwachs. Dies werden primär der Oxidation von Sulfid zu Kupfer(I)-oxid und der Bildung von Kupfer(II)-sulfat zugeschrieben. Danach verlangsamt sich die Reaktion, jedoch setzte bei 490°C das Schmelzen ein, was eine weitere Oxidation ermöglicht, die sich mit einer zweiten Exothermen und Massensteigerung zeigte. Bei 570°C ist die Sulfid-Oxidation abgeschlossen, jedoch fanden Feststoffreaktionen zwischen Cu_2O und $CuSO_4$ statt, wobei $CuO \cdot CuSO_4$ gebildet wird. Cu_2O wird zu einem gewissen Grade umgesetzt. Bei 775°C werden nur die beiden Phasen CuO und $CuO \cdot CuSO_4$ beobachtet. Oberhalb dieser Temperatur ist letztere Phase unbeständig und wird zum Endprodukt CuO zersetzt.